JOURNAL OF GUIDANCE, CONTROL, AND DYNAMICS
Vol. 28, No. 4, July–August 2005

Robustness Analysis of Nonlinear Flight Controllers

Christakis Papageorgiou* and Keith Glover†
Cambridge University, Cambridge, England CB2 1PZ, United Kingdom

The development of robustness analysis tests is presented for quasi-linear-parameter-varying models in the presence of time-varying, parametric uncertainty. The tests are applied for the robustness analysis of nonlinear dynamic inversion control laws giving sufficient conditions for assessing the nonlinear system's performance in the presence of bounded disturbances and uncertainty. The tests are formulated as linear minimisation problems subject to linear matrix inequality constraints and solved by using a gridding procedure. A detailed example is presented in which two nonlinear dynamic inversion control laws for the short-period dynamics of an aircraft are analysed and compared.

I. Introduction

THE application of nonlinear dynamic inversion techniques in flight control has been popular in recent years.[1–4] This design technique uses the information about the nonlinear dynamics of the aircraft in the process of designing the control law. The resulting nonlinear controller is valid for the whole of the flight envelope without having the need to apply gain scheduling techniques between for example various linear controllers.

Other attractive features of this design technique are as follows: 1) the decoupling of the chosen variables to be controlled after the inversion is applied, which allows the decoupling of the longitudinal from the lateral dynamics at high-angle-of-attack flight[5]; 2) the independent assignment of closed-loop dynamics on each output channel[6]; and 3) the simplicity in designing the controller and the simple structure of the controller, which is based on state feedback and allows the designer to have an insight on how the controller behaves. The theoretical background on nonlinear dynamic inversion (NDI) or feedback linearization is addressed in Ref. 7. The application of NDI is demonstrated on the following nonlinear, single-input single-output system:

$$\dot{\boldsymbol{x}} = f(\boldsymbol{x}) + g(\boldsymbol{x})u, \qquad \boldsymbol{x} \in \mathbb{R}^n \tag{1}$$

$$y = h(\boldsymbol{x}) \tag{2}$$

The output to be controlled y is differentiated until the input appears explicitly in the expression

$$\dot{y} = \frac{\partial h}{\partial \boldsymbol{x}}\dot{\boldsymbol{x}} = \frac{\partial h}{\partial \boldsymbol{x}} f(\boldsymbol{x}) + \frac{\partial h}{\partial \boldsymbol{x}} g(\boldsymbol{x})u \tag{3}$$

Assuming that the inverse of $(\partial h/\partial \boldsymbol{x})g(\boldsymbol{x})$ exists for all $\boldsymbol{x} \in \mathbb{R}^n$, the use of the state feedback

$$u = \left[\frac{\partial h}{\partial \boldsymbol{x}} g(\boldsymbol{x})\right]^{-1}\left[v - \frac{\partial h}{\partial \boldsymbol{x}} f(\boldsymbol{x})\right], \qquad \text{(NDI inner loop)} \tag{4}$$

results in an integrator response from the external input v to the output y. Using either one of the linear, outer-loop control laws

$$v = \omega_y(y_{\text{dem}} - y), \qquad v = \omega_y y_{\text{dem}} - 2\omega_y y + \omega_y^2 \int_0^t (y_{\text{dem}} - y)\,\mathrm{d}t \tag{5}$$

results in the following input-output response:

$$\dot{y} + \omega_y y = \omega_y y_{\text{dem}} \tag{6}$$

Although the input-output response is feedback linearized, there exist certain dynamics that are unobservable at the output and exhibit nonlinear behavior. These are called zero dynamics and constitute a limitation of NDI because for example they end up being unstable when NDI is applied to nonminimum phase systems.[8]

The main disadvantage of NDI is that it does not provide a priori any robustness guarantees for the closed-loop system, thus making the flight clearance procedure a crucial step in the development of the control law. The clearance procedure demonstrates to the aviation authorities that a control law will function in a satisfactory way for a given flight envelope and in the presence of failure conditions and uncertainty. Major sources of uncertainty in modeling rigid aircraft dynamics are caused by 1) variations in parameters such as the mass and the moments of inertia resulting from different store configurations, and 2) uncertainty in the aerodynamic data resulting from a lack of knowledge regarding the effects of the nonlinear unsteady aerodynamics.

Most analysis techniques for NDI flight control laws are based on linear methods. The methodology is to linearize the nonlinear closed-loop system at various points in the flight envelope and apply linear methods to investigate the robustness of the control law. Such a procedure is presented in Ref. 9, where the robustness is investigated using gain and phase margins. The procedure can be tedious because it must be applied to all channels and for a significant number of trim points that span the flight envelope. Another linear analysis method is μ-analysis,[10] which can naturally address the issue of parametric uncertainty, that is, uncertainty in aerodynamic coefficients, mass, and moments of inertia. A recent linear analysis technique is based on the robust stability margin $b_{P,C}$, which is a consequence of the $\mathcal{H}_\infty$ loop-shaping procedure.[11,12] This technique was used in Ref. 13 for the frozen-point analysis of an NDI control law for the longitudinal rigid-body dynamics of the Harrier. It was shown in Ref. 14 how to interpret the robust stability margin $b_{P,C}$ in terms of criteria, which are currently used for the clearance of flight control laws.

The nonlinear nature of an NDI control law has motivated the examination of its stability properties in the nominal case, which amounts to checking the stability of the nonlinear zero dynamics. The authors of Ref. 15 examine the application of an inversion law on a bank-to-turn air-to-air missile. The nominal stability of an equilibrium point of the closed-loop dynamics is established using Lyapunov analysis. In Ref. 16 the authors characterize the nominal stability for a generic, pitch-axis, aircraft model in terms of certain conditions on the aerodynamic coefficients of the aircraft. Also the robust stability of the zero dynamics with respect to uncertainty in the aerodynamic coefficients is investigated. The authors assume no uncertainty on the pitch-moment coefficients, which allows the decoupling of the controlled dynamics from the zero dynamics. It is

Received 20 March 2004; revision received 3 August 2004; accepted for publication 13 September 2004.

*Research Associate, Control Group; cp206@eng.cam.ac.uk.
†Head of Department, Department of Engineering; kg@eng.cam.ac.uk.

the first result obtained on the robustness analysis of an NDI control law.

The nonlinear analysis of NDI control laws was further facilitated with the use of quasi-linear-parameter-varying (LPV)[17] models to approximate the nonlinear aircraft dynamics and with the development of numerous analysis techniques for LPV models. LPV models are linear models the state-space matrices of which depend on external, time-varying parameters, whereas in quasi-LPV models those parameters are allowed to be endogenous, that is, states of the system. Thus, the quasi-LPV framework allows the representation both of the nonlinear effects and of any parametric uncertainty. The two main tools in the analysis of LPV models are based on quadratic Lyapunov functions and parameter-dependent Lyapunov functions. A quadratic Lyapunov test is used in Ref. 18 for the robustness analysis of a missile autopilot designed with NDI. The authors examine robust stability with respect to uncertainty in the aerodynamic coefficients of the missile. A less conservative but more computationally expensive test was applied in Ref. 13 by using parameter-dependent Lyapunov functions. The authors analyzed and compared the robustness of several NDI control laws for the short-period dynamics of the Harrier.

An indicative analysis technique sometimes used for the closed-loop quasi-LPV system is to assume the scheduling variables are in fact bounded, exogenous variables. Such analysis will only be rigorous if it can be separately ensured that the scheduling variables remain within their assumed bounds. So the need arises to associate the range of the endogenous scheduling variables over which the analysis test is performed with the size of the external signals, which for closed-loop systems will be the reference commands on the controlled outputs. This will lead to local results for the analysis of the stability and performance of nonlinear systems under time-varying parametric uncertainty, which is the main contribution of this work.

The material in this paper will be presented in the following sections:

1) Section II will present a procedure for deriving a quasi-LPV model about an equilibrium point of the original, nonlinear system.

2) Section III will briefly present the notion of quadratic Lyapunov functions and their use in assessing the stability and performance of LPV models.

3) Section IV will present the tests for assessing the robust performance and robust stability of a quasi-LPV model with respect to time-varying, parametric uncertainty.

4) Section V will present the analysis and comparison of two NDI control laws for the short-period dynamics of an F/A-18 aircraft.

II. Procedure for Deriving Quasi-LPV Models

The closed-loop nonlinear system must be written as a quasi-LPV model to apply the robustness tests. A technique for transforming a nonlinear model into a quasi-LPV model was proposed in Ref. 19, which relies on the existence of a family of equilibrium points that is parameterized by the scheduling variables. The procedure proposed here only deals with a single equilibrium point of the nonlinear system:

$$\dot{\boldsymbol{x}} = f(\boldsymbol{x}) + \sum_{i=1}^{n_u} g_i(\boldsymbol{x})u_i, \qquad \boldsymbol{x} \in \boldsymbol{D} \subset \mathbb{R}^n, \qquad \boldsymbol{u} \in \mathbb{R}^{n_u} \tag{7}$$

$$\boldsymbol{y} = h(\boldsymbol{x}), \qquad \boldsymbol{y} \in \mathbb{R}^{n_y} \tag{8}$$

The vector fields $f(\boldsymbol{x})$, $h(\boldsymbol{x})$, and $g_i(\boldsymbol{x})$ are rational functions of $\boldsymbol{x}$ (element wise). It is assumed that there exists a unique equilibrium point $(\boldsymbol{x}_0, \boldsymbol{u}_0)$ associated with the nonlinear system that satisfies

$$f(\boldsymbol{x}_0) + \sum_{i=1}^{n_u} g_i(\boldsymbol{x}_0)u_{0_i} = 0, \qquad \boldsymbol{x}_0 \in \boldsymbol{D} \tag{9}$$

$$\boldsymbol{y}_0 = h(\boldsymbol{x}_0) \tag{10}$$

The first step in obtaining the quasi-LPV model is to subtract the equilibrium condition from the original nonlinear equations. Subtracting Eq. (9) from Eq. (7) results in

$$\dot{\boldsymbol{x}} = f(\boldsymbol{x}) - f(\boldsymbol{x}_0) + \sum_{i=1}^{n_u} \left[g_i(\boldsymbol{x})u_i - g_i(\boldsymbol{x}_0)u_{0_i} \right] \Rightarrow \dot{\boldsymbol{x}} = f(\boldsymbol{x})$$

$$- f(\boldsymbol{x}_0) + \sum_{i=1}^{n_u} \left\{ g_i(\boldsymbol{x})\left(u_i - u_{0_i}\right) + [g_i(\boldsymbol{x}) - g_i(\boldsymbol{x}_0)]u_{0_i} \right\} \tag{11}$$

The next step is to decompose the rational functions as

$$f(\boldsymbol{x}) - f(\boldsymbol{x}_0) = F(\boldsymbol{x}, \boldsymbol{x}_0)(\boldsymbol{x} - \boldsymbol{x}_0), \qquad F(\boldsymbol{x}, \boldsymbol{x}_0) \in \mathbb{R}^{n \times n} \tag{12}$$

$$[g_i(\boldsymbol{x}) - g_i(\boldsymbol{x}_0)]u_{0_i} = G_i(\boldsymbol{x}, \boldsymbol{x}_0)u_{0_i}(\boldsymbol{x} - \boldsymbol{x}_0)$$

$$G_i(\boldsymbol{x}, \boldsymbol{x}_0) \in \mathbb{R}^{n \times n}, \qquad i = 1, \ldots, n_u \tag{13}$$

This creates new state variables, which are the deviations of the actual states from their equilibrium values, and new input variables, which are the deviations of the actual inputs from their equilibrium values. It was shown in Ref. 20 that this decomposition is not unique when $n > 1$. As an example of the nonuniqueness of this decomposition, consider

$$2x_1x_2 - 2x_{1_0}x_{2_0} = \begin{bmatrix} 2x_2 & 2x_{1_0} \end{bmatrix} \begin{bmatrix} x_1 - x_{1_0} \\ x_2 - x_{2_0} \end{bmatrix}$$

$$= \begin{bmatrix} 2x_{2_0} & 2x_1 \end{bmatrix} \begin{bmatrix} x_1 - x_{1_0} \\ x_2 - x_{2_0} \end{bmatrix} \tag{14}$$

Substituting Eqs. (12) and (13) back in Eq. (11), we get

$$\dot{\boldsymbol{x}} = \left[F(\boldsymbol{x}, \boldsymbol{x}_0) + \sum_{i=1}^{n_u} G_i(\boldsymbol{x}, \boldsymbol{x}_0)u_{0_i} \right](\boldsymbol{x} - \boldsymbol{x}_0) + \sum_{i=1}^{n_u} g_i(\boldsymbol{x})(u_i - u_{0_i}) \tag{15}$$

Following the same steps with the output equation will result in

$$\boldsymbol{y} - \boldsymbol{y}_0 = H(\boldsymbol{x}, \boldsymbol{x}_0)(\boldsymbol{x} - \boldsymbol{x}_0) \tag{16}$$

By redefining the variables as $\Delta\boldsymbol{x} = \boldsymbol{x} - \boldsymbol{x}_0$, $\Delta u_i = u_i - u_{0_i}$, and $\Delta\boldsymbol{y} = \boldsymbol{y} - \boldsymbol{y}_0$, we have

$$\Delta\dot{\boldsymbol{x}} = \left[F(\boldsymbol{x}, \boldsymbol{x}_0) + \sum_{i=1}^{n_u} G_i(\boldsymbol{x}, \boldsymbol{x}_0)u_{0_i} \right]\Delta\boldsymbol{x} + \sum_{i=1}^{n_u} g_i(\boldsymbol{x})\Delta u_i \tag{17}$$

$$\Delta\boldsymbol{y} = H(\boldsymbol{x}, \boldsymbol{x}_0)\Delta\boldsymbol{x} \tag{18}$$

The derivation of the quasi-LPV model involves no loss of information regarding the nonlinear dynamics and is associated with the equilibrium point $(\boldsymbol{x}_0, \boldsymbol{u}_0)$. It is shown in Ref. 21 that the frozen, quasi-LPV model which is obtained by setting $\boldsymbol{x} = \boldsymbol{x}_0$ in Eqs. (17) and (18) is the same as the linear model that would have been obtained from a Taylor-series expansion of the nonlinear equation (7) about its equilibrium point $(\boldsymbol{x}_0, \boldsymbol{u}_0)$. When freezing the state of the quasi-LPV model at its equilibrium value, the signals $\Delta\boldsymbol{x}$, $\Delta\boldsymbol{u}$, and $\Delta\boldsymbol{y}$ become small deviations of the respective variables from their equilibrium values.

The proposed procedure allows all of the state variables to be scheduling variables as opposed to the procedure in Ref. 19, which only considers the scheduling variables to be a subset of the state vector and furthermore restricts the scheduling variables to be the controlled outputs. Subsequently the procedure in Ref. 19 deals only with output-nonlinear systems whose state-space representation is given by

$$\begin{bmatrix} \dot{\boldsymbol{z}} \\ \dot{\boldsymbol{w}} \end{bmatrix} = f(\boldsymbol{z}) + A(\boldsymbol{z}) \begin{bmatrix} \boldsymbol{z} \\ \boldsymbol{w} \end{bmatrix} + B(\boldsymbol{z})\boldsymbol{u} \tag{19}$$

On the other hand, the procedure in Ref. 19 allows the representation of the nonlinear dynamics over a family of equilibrium points that is parameterized by the scheduling variable z, which is more advantageous than the procedure proposed in this paper, which considers the nonlinear dynamics about a single equilibrium point.

The proposed method was initially introduced in Ref. 22, and in Ref. 23 it was applied on the nonlinear model of Eq. (19), where greater detail has been given on how to apply the decomposition of the nonlinear functions after the subtraction of the trim point condition from the original nonlinear equations.

The proposed technique was applied in Ref. 21 for the development of a quasi-LPV model for the short-period dynamics of an F/A-18 aircraft.

III. Quadratic Lyapunov Functions for the Analysis of LPV Models

Lyapunov functions are used for the stability analysis of nonlinear systems using Lyapunov's stability theorem,[24] which gives a sufficient condition for testing the asymptotic stability of the equilibrium point of a nonlinear system, and it provides a means of calculating a region that is a subset of the region of attraction. One procedure to find a Lyapunov function $V(\boldsymbol{x})$ is to choose a Lyapunov function candidate with free parameters and adjust those parameters to satisfy $V(\boldsymbol{x}) > 0$ and $\dot{V}(\boldsymbol{x}) < 0$. An example is the quadratic Lyapunov function $V(\boldsymbol{x}) = \boldsymbol{x}^T P \boldsymbol{x}$, where a positive-definite symmetric matrix P is sought to satisfy

$$\dot{V}(\boldsymbol{x}) = \dot{\boldsymbol{x}}^T P \boldsymbol{x} + \boldsymbol{x}^T P \dot{\boldsymbol{x}} < 0 \tag{20}$$

Quadratic Lyapunov functions are widely used in the stability and performance analysis of LPV systems under the name of quadratic stability.[25]

Definition 2.1 (LPV system[26]): Given a compact subset $\boldsymbol{P} \subset \mathbb{R}^s$, the parameter variation set $\boldsymbol{F}_P$ denotes the set of all piecewise continuous functions mapping time into $\boldsymbol{P}$ with a finite number of discontinuities in any interval. Given $\boldsymbol{P} \subset \mathbb{R}^s$, the continuous functions $A : \mathbb{R}^s \to \mathbb{R}^{n \times n}$, $B : \mathbb{R}^s \to \mathbb{R}^{n \times n_d}$, $C : \mathbb{R}^s \to \mathbb{R}^{n_e \times n}$, and $D : \mathbb{R}^s \to \mathbb{R}^{n_e \times n_d}$ represent an nth-order, LPV system, whose dynamics evolve as

$$\begin{bmatrix} \dot{\boldsymbol{x}} \\ \boldsymbol{e} \end{bmatrix} = \begin{bmatrix} A(\boldsymbol{\rho}(t)) & B(\boldsymbol{\rho}(t)) \\ C(\boldsymbol{\rho}(t)) & D(\boldsymbol{\rho}(t)) \end{bmatrix} \begin{bmatrix} \boldsymbol{x} \\ \boldsymbol{d} \end{bmatrix}, \qquad \text{where} \quad \boldsymbol{\rho}(t) \in \boldsymbol{F}_P \tag{21}$$

For any $\boldsymbol{\rho}(t) \in \boldsymbol{F}_P$, the causal, linear operator G_ρ is defined by

$$\boldsymbol{e}(t) = G_\rho(\boldsymbol{d})(t) := \int_0^t C(\boldsymbol{\rho}(\tau))\Phi_\rho(t,\tau)B(\boldsymbol{\rho}(\tau))\boldsymbol{d}(\tau)\,\mathrm{d}\tau + D(\boldsymbol{\rho}(t))\boldsymbol{d}(t) \tag{22}$$

where $\Phi_\rho(t, t_0)$ is the state-transition matrix.

Definition 2.2 (quadratic stability): The undriven LPV system $\dot{\boldsymbol{x}} = A(\boldsymbol{\rho}(t))\boldsymbol{x}$ is quadratically stable over $\boldsymbol{P}$ if there exists a $P \in \mathbb{R}^{n \times n}$, $P = P^T > 0$ such that

$$A^T(\boldsymbol{\rho})P + PA(\boldsymbol{\rho}) < 0, \qquad \forall \boldsymbol{\rho} \in \boldsymbol{P} \tag{23}$$

Because A depends continuously on $\boldsymbol{\rho} \in \boldsymbol{P}$ and $\boldsymbol{P}$ is compact, condition (23) implies that for any $\boldsymbol{\rho}(t) \in \boldsymbol{F}_P$,

$$\dot{V}(\boldsymbol{x}) = \boldsymbol{x}^T[A^T(\boldsymbol{\rho}(t))P + PA(\boldsymbol{\rho}(t))]\boldsymbol{x} < 0 \tag{24}$$

which further implies[26] that for any $\boldsymbol{\rho}(t) \in \boldsymbol{F}_P$ there exist positive constants k and γ such that

$$\|\Phi_\rho(t, t_0)\| \le ke^{-\gamma(t-t_0)}, \qquad \forall t \ge t_0 \tag{25}$$

It is shown in Ref. 24 that condition (25) is equivalent to the equilibrium point $\boldsymbol{x} = 0$ of the undriven LPV system being uniformly asymptotically stable for any $\boldsymbol{\rho}(t) \in \boldsymbol{F}_P$. The performance of a quadratically stable LPV system is examined using the $\mathcal{L}_2$-induced gain from inputs to outputs.

Definition 2.3 ($\mathcal{L}_2$-induced gain of an LPV system[26]): For the quadratically stable LPV system of Eq. (21) with zero initial conditions, the $\mathcal{L}_2$-induced gain is defined as

$$\sup_{\boldsymbol{\rho}(t) \in \boldsymbol{F}_P} \sup_{\boldsymbol{d} \in \mathcal{L}_2} \frac{\|\boldsymbol{e}\|_2}{\|\boldsymbol{d}\|_2} \tag{26}$$

It signifies the largest energy gain from inputs to outputs over all of the allowable parameter trajectories. It is used as a measure of performance because it can place an upper bound on the energy of a performance output in response to excitation from either a reference input or an external disturbance. The following theorem from Ref. 26 gives a sufficient condition in terms of an linear matrix inequality (LMI) for bounding the $\mathcal{L}_2$-induced gain of an LPV system.

Theorem 2.1 (bound on the $\mathcal{L}_2$-induced gain of an LPV system): The LPV system in Eq. (21) with $D(\boldsymbol{\rho}(t)) = 0$ is quadratically stable and its $\mathcal{L}_2$-induced gain is less than γ if there exists a $P = P^T > 0$ such that

$$\begin{bmatrix} A^T(\boldsymbol{\rho})P + PA(\boldsymbol{\rho}) + C^T(\boldsymbol{\rho})C(\boldsymbol{\rho}) & PB(\boldsymbol{\rho}) \\ B^T(\boldsymbol{\rho})P & -\gamma^2 I \end{bmatrix} < 0, \qquad \forall \rho \in \boldsymbol{P} \tag{27}$$

The LMI in Eq. (27) is a consequence of the search for a Lyapunov function $V(\boldsymbol{x}) = \boldsymbol{x}^T P \boldsymbol{x}$ so that

$$\dot{V}(\boldsymbol{x}) + \boldsymbol{e}^T\boldsymbol{e} - \gamma^2\boldsymbol{d}^T\boldsymbol{d} < 0$$

$$\forall \boldsymbol{x}, \boldsymbol{d} \quad \text{satisfying Eq. (21)} \quad \text{with} \quad \boldsymbol{x}(0) = 0 \tag{28}$$

For a quasi-LPV model the matrices $A()$, $B()$, $C()$ will also be functions of the endogenous scheduling variables, which will be assumed a priori to vary in a given range. In that case we need an indication of whether the trajectory of the scheduling variables will remain in that range for a reference input of a given size. This leads to the notion of a set of reachable states for the LPV system in Eq. (21) and of ways to bound this set using ellipsoids.

Definition 2.4 (set of reachable states[25]): The set of reachable states of the LPV model in Eq. (21) under unit-energy inputs is given by all $\boldsymbol{x}(T)$ that satisfy

$$\dot{\boldsymbol{x}} = A(\boldsymbol{\rho}(t))\boldsymbol{x} + B(\boldsymbol{\rho}(t))\boldsymbol{d}$$

$$\boldsymbol{\rho}(t) \in \boldsymbol{F}_P, \qquad \boldsymbol{x}(0) = 0, \qquad \int_0^T \boldsymbol{d}^T\boldsymbol{d}\,\mathrm{d}t \le 1 \tag{29}$$

Suppose there exists a Lyapunov function $V(\boldsymbol{x}) = \boldsymbol{x}^T P \boldsymbol{x}$ and a real number c that satisfy

$$\dot{V}(\boldsymbol{x}) \le c^2\boldsymbol{d}^T\boldsymbol{d}, \qquad \forall \boldsymbol{x}, \boldsymbol{d} \quad \text{that satisfy Eq. (29)} \tag{30}$$

Integrating from 0 to t where $0 < t \le T$, we get

$$\boldsymbol{x}^T(t)P\boldsymbol{x}(t) \le c^2 \int_0^t \boldsymbol{d}^T\boldsymbol{d}\,\mathrm{d}t \le c^2 \int_0^T \boldsymbol{d}^T\boldsymbol{d}\,\mathrm{d}t \le c^2 \tag{31}$$

This implies that for any $T > 0$ and any unit-energy input the set of reachable states is contained in the ellipsoid $\mathcal{E}(P, c)$, where the ellipsoid is defined as

$$\mathcal{E}(P, c) := \{\boldsymbol{x} \in \mathbb{R}^n : \boldsymbol{x}^T P \boldsymbol{x} \le c^2\} \tag{32}$$

Next we will extend the results of this section to characterize the robust stability and robust performance of quasi-LPV models.

IV. Robustness Analysis of Quasi-LPV Models

Uncertain, quasi-LPV models can be obtained from LPV models by considering

$$\boldsymbol{\rho}(t) = [\boldsymbol{x}^T(t) \quad \boldsymbol{\delta}^T(t)]^T \tag{33}$$

The parameter vector $\boldsymbol{\rho}(t)$ is separated in the endogenous scheduling variables $\boldsymbol{x}(t)$ that capture the nonlinear behavior and the external uncertain parameters $\boldsymbol{\delta}(t)$ that describe the uncertainty.

A. Robust Stability of Quasi-LPV Models

The notion of quadratic stability can be used to examine the local stability of the equilibrium point of the undriven, uncertain, quasi-LPV model,

$$\dot{\boldsymbol{x}} = A(\boldsymbol{x}(t), \boldsymbol{\delta}(t))\,\boldsymbol{x}, \qquad \boldsymbol{x} \in \boldsymbol{D} \subset \mathbb{R}^n, \qquad \boldsymbol{\delta}(t) \in \boldsymbol{F}_\Delta \quad (34)$$

The sets $\boldsymbol{F}_\Delta$ and $\boldsymbol{\Delta}$ have the same meaning as those in definition 2.1 but are now referring to the uncertain parameters. Because $\boldsymbol{x}(t)$ is a priori required to vary in a domain $\boldsymbol{D}$, the quadratic stability result will have to be local and be interpreted in the form of a region of attraction of the equilibrium point.

Theorem 3.1 (robust stability of a quasi-LPV model): The equilibrium point of the undriven quasi-LPV model in Eq. (34) is asymptotically stable for any $\boldsymbol{\delta}(t) \in \boldsymbol{F}_\Delta$, if there exists $P = P^T > 0$ such that

$$A^T(\boldsymbol{x}, \boldsymbol{\delta})P + PA(\boldsymbol{x}, \boldsymbol{\delta}) < 0, \qquad \forall \boldsymbol{x} \in \boldsymbol{D}, \qquad \forall \boldsymbol{\delta} \in \boldsymbol{\Delta} \quad (35)$$

A subset of the region of attraction is given by the ellipsoid $\mathcal{E}(P, c)$ provided that the positive real number c is chosen to satisfy $\mathcal{E}(P, c) \subset \boldsymbol{D}$.

The proof is given in the Appendix as the proof of the first part of theorem 3.3. The condition $\mathcal{E}(P, c) \subset \boldsymbol{D}$ can be expressed as an LMI (see Ref. 25) if $\boldsymbol{D}$ is a polytope given by

$$\boldsymbol{D} = \left\{\boldsymbol{x} \in \mathbb{R}^n : a_k^T \boldsymbol{x} \le 1, k = 1, \ldots, q\right\} \quad (36)$$

The condition for stability (35) results in an infinite number of constraints on the symmetric matrix P. To make it numerically tractable, it is necessary to grid over the uncertain parameter space $\boldsymbol{\Delta}$ and the domain $\boldsymbol{D}$. When the matrix $A(\boldsymbol{x}, \boldsymbol{\delta})$ is an affine function of the parameter vector $\boldsymbol{\delta}$ and $\boldsymbol{\Delta}$ is a convex set, the gridding procedure over $\boldsymbol{\Delta}$ can be avoided. Let the uncertain parameter region $\boldsymbol{\Delta}$ be given by the convex set

$$\boldsymbol{\Delta} = \{\boldsymbol{\delta} : \delta_j \in [\underline{\delta}_j, \bar{\delta}_j],\ j = 1, \ldots, s\} \quad (37)$$

This results in an uncertain parameter region with a finite number of corners (2^s). Let $\boldsymbol{\Delta}_0$ be the set of corners of this region. The following theorem about affine, parameter-dependent models is presented in Ref. 27.

Theorem 3.2: For $\boldsymbol{x}_0 \in \boldsymbol{D}$, let $A(\boldsymbol{x}_0, \boldsymbol{\delta})$ be an affine function of the parameter vector $\boldsymbol{\delta} \in \boldsymbol{\Delta}$ with $\boldsymbol{\Delta}$ a convex set. Then,

$$A(\boldsymbol{x}_0, \boldsymbol{\delta})^T P + PA(\boldsymbol{x}_0, \boldsymbol{\delta}) < 0, \qquad \forall \boldsymbol{\delta} \in \boldsymbol{\Delta}$$

$$\Leftrightarrow\ A(\boldsymbol{x}_0, \boldsymbol{\delta})^T P + PA(\boldsymbol{x}_0, \boldsymbol{\delta}) < 0, \qquad \forall \boldsymbol{\delta} \in \boldsymbol{\Delta}_0 \quad (38)$$

The dependence of the matrix A on the state variable $\boldsymbol{x}$ is likely to be nonaffine because it describes the nonlinearities of the model. So the gridding of the domain $\boldsymbol{D}$ is not avoided, but usually the number of the scheduling variables (angle of attack, altitude, and speed) will be less than the external, uncertain parameters (aerodynamic coefficients, moments of inertia, mass), and hence a significant reduction in the number of LMIs is achieved.

B. Robust Performance of Quasi-LPV Models

Given the uncertain, quasi-LPV model,

$$\dot{\boldsymbol{x}} = A(\boldsymbol{x}, \boldsymbol{\delta}(t))\,\boldsymbol{x} + B(\boldsymbol{x}, \boldsymbol{\delta}(t))\boldsymbol{d}, \qquad \boldsymbol{x}(0) = 0$$

$$\boldsymbol{e} = C(\boldsymbol{x}, \boldsymbol{\delta}(t))\,\boldsymbol{x}, \qquad \boldsymbol{\delta}(t) \in \boldsymbol{F}_\Delta, \qquad \boldsymbol{x} \in \boldsymbol{D} \quad (39)$$

the performance analysis problem is formulated in two consecutive steps:

1) Bound on the scheduling variables: Calculate the maximum $\mathcal{L}_2$ norm of the external input $\boldsymbol{d}$ for which it is guaranteed that the state remains in a given region $\hat{\boldsymbol{D}} \subset \boldsymbol{D}$ for any $\boldsymbol{\delta}(t) \in \boldsymbol{F}_\Delta$.

2) Bound on the $\mathcal{L}_2$-induced gain: For that class of external inputs and that amount of parametric uncertainty, calculate an upper bound on the $\mathcal{L}_2$-induced gain from the external input $\boldsymbol{d}$ to the output $\boldsymbol{e}$.

The preceding formulation of the robust performance problem of a quasi-LPV model and its solution using theorems 3.3 and 3.4 is the main contribution of this work.

Theorem 3.3 (bound on the scheduling variables): Regarding the uncertain quasi-LPV system of Eqs. (39), if there exists a $P = P^T > 0$ such that

$$\begin{bmatrix} A^T(\boldsymbol{x}, \boldsymbol{\delta})P + PA(\boldsymbol{x}, \boldsymbol{\delta}) & PB(\boldsymbol{x}, \boldsymbol{\delta}) \\ B^T(\boldsymbol{x}, \boldsymbol{\delta})P & -I \end{bmatrix} < 0$$

$$\forall \boldsymbol{\delta} \in \boldsymbol{\Delta}, \quad \forall \boldsymbol{x} \in \hat{\boldsymbol{D}} \subset \boldsymbol{D} \quad (40)$$

and if there exists a $c > 0$ such that $\mathcal{E}(P, c) \subset \hat{\boldsymbol{D}}$, then for any uncertain parameter $\boldsymbol{\delta}(t) \in \boldsymbol{F}_\Delta$, 1) the ellipsoid $\mathcal{E}(P, c)$ is a subset of the region of attraction of the undriven, uncertain, quasi-LPV model $\dot{\boldsymbol{x}} = A(\boldsymbol{x}(t), \boldsymbol{\delta}(t))\,\boldsymbol{x}$; and 2) every trajectory of Eqs. (39) with $\boldsymbol{x}(0) = 0$ and for any input $\boldsymbol{d}$ that satisfies $\|\boldsymbol{d}\|_2^2 < c^2$ is guaranteed to stay in $\mathcal{E}(P, c)$ and hence in $\hat{\boldsymbol{D}}$.

Condition (40) is a parameter-dependent LMI that can be made numerically tractable by the gridding of $\hat{\boldsymbol{D}}$ and by the convexity argument of theorem 3.2. The condition $\mathcal{E}(P, c) \subset \hat{\boldsymbol{D}}$ can be written as an LMI in P and $1/c^2$. Given the size of $\hat{\boldsymbol{D}}$, we would like to calculate the "largest" set of external inputs for which it is guaranteed that the state remains in $\hat{\boldsymbol{D}}$. Thus, the problem of calculating the maximum energy of the external input is formulated as a minimization of a linear cost function subject to LMIs and can be solved efficiently using the LMI toolbox.[28] It is assumed that the region $\hat{\boldsymbol{D}}$ is a symmetric region about the equilibrium point $\boldsymbol{x} = 0$ with respect to each state, and the optimization problem is solved for increasing sizes of $\hat{\boldsymbol{D}}$. The problem of calculating an upper bound on the $\mathcal{L}_2$-induced gain is addressed in the following theorem.

Theorem 3.4 (bound on the $\mathcal{L}_2$-induced gain): Given c as the solution of the problem in theorem 3.3, if there exists a $P = P^T > 0$ and $\gamma > 0$ such that

$$\begin{bmatrix} A^T(\boldsymbol{x}, \boldsymbol{\delta})P + PA(\boldsymbol{x}, \boldsymbol{\delta}) + C^T(\boldsymbol{x}, \boldsymbol{\delta})C(\boldsymbol{x}, \boldsymbol{\delta}) & PB(\boldsymbol{x}, \boldsymbol{\delta}) \\ B^T(\boldsymbol{x}, \boldsymbol{\delta})P & -\gamma^2 I \end{bmatrix} < 0$$

$$\forall \boldsymbol{\delta} \in \boldsymbol{\Delta}, \quad \forall \boldsymbol{x} \in \hat{\boldsymbol{D}} \quad (41)$$

then the $\mathcal{L}_2$-induced gain from $\boldsymbol{d}$ to $\boldsymbol{e}$ is less than γ for any $\boldsymbol{\delta}(t) \in \boldsymbol{F}_\Delta$ and for any input such that $\|\boldsymbol{d}\|_2^2 < c^2$.

The proof of theorems 3.3 and 3.4 is given in the Appendix.

The quasi-LPV model in Eq. (39) can be considered as the closed-loop system obtained from the application of an NDI control law on the uncertain, nonlinear equations of an aircraft. The parameter $\boldsymbol{\delta}(t)$ is an uncertain, time-varying parameter that is not measured as opposed to the scheduling variable $\boldsymbol{x}$, which is fully measured.

The results of theorems 3.3 and 3.4 imply that for a given amount of uncertainty and for external inputs of bounded energy the energy of the output will be less than a certain value. This is a local result associated with a region in the state space that is guaranteed to contain the state trajectory for the specific amount of uncertainty and amount of energy in the reference input.

V. Analysis of an NDI Control Law for the F/A-18 Short-Period Dynamics

The short-period dynamics can be physically described by using only the pitch-rate and angle-of-attack variables while the speed and altitude are fairly constant.[29] The short-period dynamics evolve on a much faster timescale than the phugoid-mode dynamics (involving speed and altitude). A quasi-LPV model approximating the F/A-18 short-period dynamics is derived in Ref. 21 from a nonlinear, aeroservoelastic F/A-18 model provided by QinetiQ[30] and shown next:

$$\begin{bmatrix} \dot{q} \\ \Delta\dot{\alpha} \end{bmatrix} = \begin{bmatrix} 0 & \dfrac{1}{I_{yy}} M_\alpha(\alpha) \\ 1 + \dfrac{\cos(\alpha)}{mV_0} Z_q(\alpha) & \dfrac{\cos(\alpha)}{mV_0} Z_\alpha(\alpha) \end{bmatrix} \begin{bmatrix} q \\ \Delta\alpha \end{bmatrix} + \begin{bmatrix} \dfrac{1}{I_{yy}} M_\epsilon(\alpha) \\ \dfrac{\cos(\alpha)}{mV_0} Z_\epsilon(\alpha) \end{bmatrix} \Delta\epsilon \quad (42)$$

The symbols q and α represent the pitch rate and the angle of attack, respectively, and ϵ is the elevator deflection. The symbols I_{yy} and m are the moment of inertia and the mass of the aircraft, respectively. The model is valid for an equilibrium point characterized by the speed V_0 and altitude h_0. The signals $\Delta\alpha = \alpha - \alpha_0$ and $\Delta\epsilon = \epsilon - \epsilon_0$ represent large deviations from the equilibrium values α_0 and ϵ_0. An NDI control law will be designed for the pitch-rate control of the aircraft. The aerodynamic coefficients are not known precisely, and the control law is derived based on the nominal quasi-LPV model. The robust stability and robust performance of the closed-loop system will be investigated under the presence of this parametric uncertainty using the tests derived in the preceding section.

A. Representation of Uncertainty in Aerodynamic Coefficients

The terms $M_\alpha(\alpha), \ldots, Z_\epsilon(\alpha)$ are polynomial functions of α and were obtained with a least-squares fitting on the raw data of the aerodynamics look-up table.[21] They give the amount of pitching moment or force produced as a result of a change in either the pitch rate, the angle of attack, or the elevator deflection. In this way it is easier to quantify any uncertainty on the model by considering it as uncertainty on the pitching moment and force caused by changes in the state and input variables. The uncertainty will be represented in the form of weighted, additive uncertainty on the aerodynamic coefficients as shown here:

$$
\begin{aligned}
M_\alpha(\alpha)_{\text{unc}} &= M_\alpha(\alpha) + \hat{M}_\alpha w_{M_\alpha}\delta_{M_\alpha}\\
M_\epsilon(\alpha)_{\text{unc}} &= M_\epsilon(\alpha) + \hat{M}_\epsilon w_{M_\epsilon}\delta_{M_\epsilon}\\
Z_q(\alpha)_{\text{unc}} &= Z_q(\alpha) + \hat{Z}_q w_{Z_q}\delta_{Z_q}\\
Z_\alpha(\alpha)_{\text{unc}} &= Z_\alpha(\alpha) + \hat{Z}_\alpha w_{Z_\alpha}\delta_{Z_\alpha}\\
Z_\epsilon(\alpha)_{\text{unc}} &= Z_\epsilon(\alpha) + \hat{Z}_\epsilon w_{Z_\epsilon}\delta_{Z_\epsilon}
\end{aligned}
\tag{43}
$$

The w are positive numbers that characterize the amount of uncertainty, and the constant terms $\hat{M}_\alpha, \ldots, \hat{Z}_\alpha, \hat{Z}_\epsilon$ are the average moment or force over the specific range of α defined as $\hat{M}_\alpha = 0.5[\max_\alpha M_\alpha(\alpha) + \min_\alpha M_\alpha(\alpha)]$. The δ are uncertain functions of time with the constraint that $|\delta_i(t)| \le 1$. The choice for this uncertainty representation is illustrated in Fig. 1 in the plot of the coefficient $M_\epsilon(\alpha)_{\text{unc}}$. By varying w_{M_ϵ}, an uncertainty band is created in which the moment caused by the elevator deflection is allowed to vary over the specific range of α. The uncertainty in the aerodynamic coefficients is caused by measurement errors in wind-tunnel tests, errors in fitting the raw aerodynamic data, and failure to model unsteady aerodynamics effects and the dependence of the aerodynamic coefficients on the speed. Both the unsteady aerodynamic effects and the speed dependence of the aerodynamic coefficients at high speeds justify the use of time-varying, uncertain parameters. Equation (44) is the uncertain quasi-LPV model for the short-period dynamics valid for large deviations about the trim condition characterized by a speed V_0 and altitude h_0.

$$
\begin{bmatrix} \dot{q} \\ \Delta\dot{\alpha} \end{bmatrix} =
\begin{bmatrix} 0 & \dfrac{1}{I_{yy}}\left[M_\alpha(\alpha) + \hat{M}_\alpha w_{M_\alpha}\delta_{M_\alpha}\right] \\ 1 + \dfrac{\cos(\alpha)}{mV_0}\left[Z_q(\alpha) + \hat{Z}_q w_{Z_q}\delta_{Z_q}\right] & \dfrac{\cos(\alpha)}{mV_0}\left[Z_\alpha(\alpha) + \hat{Z}_\alpha w_{Z_\alpha}\delta_{Z_\alpha}\right] \end{bmatrix}
\times \begin{bmatrix} q \\ \Delta\alpha \end{bmatrix} +
\begin{bmatrix} \dfrac{1}{I_{yy}}\left[M_\epsilon(\alpha) + \hat{M}_\epsilon w_{M_\epsilon}\delta_{M_\epsilon}\right] \\ \dfrac{\cos(\alpha)}{mV_0}\left[Z_\epsilon(\alpha) + \hat{Z}_\epsilon w_{Z_\epsilon}\delta_{Z_\epsilon}\right] \end{bmatrix} \Delta\epsilon
\tag{44}
$$

B. Control Design

The NDI control law for the pitch-rate control of the nominal, quasi-LPV model is given by

$$
\Delta\epsilon = [M_\epsilon(\alpha)/I_{yy}]^{-1}\{v - [M_\alpha(\alpha)/I_{yy}]\Delta\alpha\} \tag{45}
$$

The external signal v is the commanded pitch acceleration. Application of Eq. (45) in Eq. (44) results in the equation of the inverted, uncertain, quasi-LPV model

$$
\begin{pmatrix} \dot{q} \\ \Delta\dot{\alpha} \end{pmatrix} = A_{\text{inv}}(\alpha, \boldsymbol{\delta}) \begin{pmatrix} q \\ \Delta\alpha \end{pmatrix} + B_{\text{inv}}(\alpha, \boldsymbol{\delta})v \tag{46}
$$

where $\boldsymbol{\delta} = [\delta_{M_\alpha}\ \ \delta_{M_\epsilon}\ \ \delta_{Z_q}\ \ \delta_{Z_\alpha}\ \ \delta_{Z_\epsilon}]^T$ and $A_{\text{inv}}(\alpha, \boldsymbol{\delta})$, $B_{\text{inv}}(\alpha, \boldsymbol{\delta})$ are given, respectively, by

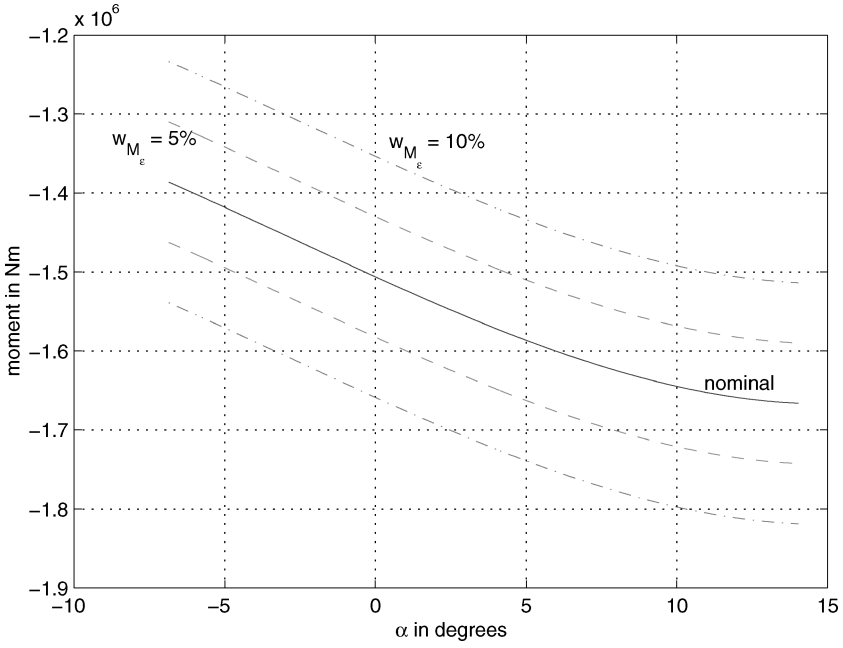

Fig. 1 Quantifying the uncertainty in the aerodynamic coefficient $M_\epsilon(\alpha)$.

$$\begin{bmatrix} 0 & \dfrac{1}{I_{yy}}\left[\hat{M}_\alpha w_{M_\alpha}\delta_{M_\alpha} - \dfrac{M_\alpha(\alpha)}{M_\epsilon(\alpha)}\hat{M}_\epsilon w_{M_\epsilon}\delta_{M_\epsilon}\right] \\ 1+\dfrac{\cos\alpha}{mV_0}\left[Z_q(\alpha)+w_{Z_q}\delta_{Z_q}\hat{Z}_q\right] & \dfrac{\cos\alpha}{mV_0}\left\{Z_\alpha(\alpha)+\hat{Z}_\alpha w_{Z_\alpha}\delta_{Z_\alpha} - \dfrac{M_\alpha(\alpha)}{M_\epsilon(\alpha)}\left[Z_\epsilon(\alpha)+\hat{Z}_\epsilon w_{Z_\epsilon}\delta_{Z_\epsilon}\right]\right\} \end{bmatrix} \begin{bmatrix} 1+w_{M_\epsilon}\delta_{M_\epsilon}\dfrac{\hat{M}_\epsilon}{M_\epsilon(\alpha)} \\ \dfrac{I_{yy}\cos\alpha}{mV_0M_\epsilon(\alpha)}\left[Z_\epsilon(\alpha)+\hat{Z}_\epsilon w_{Z_\epsilon}\delta_{Z_\epsilon}\right] \end{bmatrix}$$

For nominal conditions ($\boldsymbol{\delta}=0$), the transfer function from the input v to the pitch rate q is an integrator. In that case the pitch-rate equation does not depend on α. The $\Delta\alpha$ dynamics are the zero dynamics, and their stability is determined by the following equation:

$$\Delta\dot{\alpha} = (\cos\alpha/mV_0)\{Z_\alpha(\alpha) - [Z_\epsilon(\alpha)/M_\epsilon(\alpha)]M_\alpha(\alpha)\}\Delta\alpha \quad (47)$$

It makes sense to apply the inversion technique only if the zero dynamics are nominally stable and well behaved, because an outer-loop controller that only uses measurement of the pitch rate will not be able to stabilize these dynamics if they are unstable. Therefore it is assumed that Eq. (47) has an asymptotically stable equilibrium point $\alpha=\alpha_0$. A necessary and sufficient condition for this to hold is

$$Z_\alpha(\alpha_0)M_\epsilon(\alpha_0) < M_\alpha(\alpha_0)Z_\epsilon(\alpha_0) \quad (48)$$

Based on the assumption that the inversion is perfect, an outer-loop controller presented next is designed to stabilize the integrator response and achieve good handling qualities for the nominal, pitch-rate response.

$$\dot{\boldsymbol{x}}_k = A_k\boldsymbol{x}_k + \begin{bmatrix} B_{k_q} & B_{k_{q_{\text{com}}}} \end{bmatrix}\begin{bmatrix} q \\ q_{\text{com}} \end{bmatrix}, \qquad \boldsymbol{x}_k \in \mathbb{R}^{n_k}$$

$$v = C_k\boldsymbol{x}_k + \begin{bmatrix} D_{k_q} & D_{k_{q_{\text{com}}}} \end{bmatrix}\begin{bmatrix} q \\ q_{\text{com}} \end{bmatrix} \quad (49)$$

Substituting the controller equations in Eq. (46), the uncertain closed-loop system equation is given by

$$\dot{\boldsymbol{x}}_{\text{cl}} = A_{\text{cl}}(\alpha,\boldsymbol{\delta})\boldsymbol{x}_{\text{cl}} + B_{\text{cl}}(\alpha,\boldsymbol{\delta})q_{\text{com}}, \qquad q = C_{\text{cl}}\boldsymbol{x}_{\text{cl}} \quad (50)$$

with the following applying:

$$A_{\text{cl}}(\alpha,\boldsymbol{\delta}) = \left[\begin{array}{c|c} A_{\text{inv}}(\alpha,\boldsymbol{\delta}) + \begin{bmatrix} B_{\text{inv}}(\alpha,\boldsymbol{\delta})D_{k_q} & 0_{2\times 1} \end{bmatrix} & B_{\text{inv}}(\alpha,\boldsymbol{\delta})C_k \\ \hline \begin{bmatrix} B_{k_q} & 0_{n_k\times 1} \end{bmatrix} & A_k \end{array}\right]$$

$$B_{\text{cl}}(\alpha,\boldsymbol{\delta}) = \begin{bmatrix} B_{\text{inv}}(\alpha,\boldsymbol{\delta})D_{k_{q_{\text{com}}}} \\ B_{k_{q_{\text{com}}}} \end{bmatrix}$$

$$C_{\text{cl}} = \begin{bmatrix} 1 & 0 & 0_{1\times n_k} \end{bmatrix}, \qquad \boldsymbol{x}_{\text{cl}} = \begin{bmatrix} q & \Delta\alpha & \boldsymbol{x}_k^T \end{bmatrix}^T$$

Equation (50) is a quasi-LPV model representing the closed-loop interconnection of the NDI control law with the uncertain, short-period dynamics. It has a scheduling variable, which is the angle of attack and an uncertain parameter vector $\boldsymbol{\delta}$ that represents aerodynamic uncertainty. The angle of attack is a real, time-varying parameter assumed to vary in $\alpha\in[-5\text{ deg}, 14\text{ deg}]$ and describes the nonlinearity of the short-period mode.

C. Comparing the Robust Stability of Two NDI Control Laws

The robust stability of the undriven part of the quasi-LPV model in Eqs. (50) will be examined when employing two NDI control laws that differ only in their outer-loop control laws. One is based on proportional control, $v=\omega_q(q_{\text{com}}-q)$. The other is a proportional-plus-integral controller (PI),

$$v = \omega_q q_{\text{com}} - 2\omega_q q + \omega_q^2\int_0^t (q_{\text{com}}-q)\,\mathrm{d}t$$

The proportional control relies on the perfect inversion of the NDI controller, whereas the PI controller has an explicit integrator to account for any mismatch in the inversion as a result of uncertainties. The gain ω_q is chosen so that the nominal input-output response is $q(s)/q_{\text{com}}(s)=5/(s+5)$ in both cases. The input-output response is first order even with the explicit integrator of the PI controller as a result of the feed-forward term in the controller from q_{com}. The robust stability problem is posed as a maximization of the area of the ellipsoid that is contained in the region of attraction over the given range of α and for a given amount of uncertainty in the aerodynamic coefficients.

The robust stability tests are performed at the trim point characterised by $V_0=150$ m/s and sea-level altitude. Figure 2 shows the maximum area ellipsoids that are contained in the region of attraction for different uncertainty weights for the PI outer-loop controller. It is assumed that the uncertainty weights are equal ($w_{M_\alpha}=w_{M_\epsilon}=\cdots=w_{Z_\epsilon}=w$). The ellipsoids are obtained by solving the LMI problem,

$$\min_{P>0}\ \text{trace}\left\{\begin{bmatrix} I_2 & 0_{2\times 1} \end{bmatrix} P \begin{bmatrix} I_2 \\ 0_{2\times 1} \end{bmatrix}\right\}$$

$$A_{\text{cl}}(\alpha,\boldsymbol{\delta})^T P + P A_{\text{cl}}(\alpha,\boldsymbol{\delta}) < 0, \qquad \forall\boldsymbol{\delta}\in\boldsymbol{\Delta}_0, \qquad \forall\alpha\in[\alpha_{\min},\alpha_{\max}]$$

$$\mathcal{E}(P,1)\subset[\alpha_{\min},\alpha_{\max}]$$

The ellipsoids are contained in the domain over which the scheduling variable is varying, and they become smaller as the amount of uncertainty is increased, which means that the designer can guarantee a smaller safety region of operation for the aircraft for increasing uncertainty in the aerodynamic coefficients.

A comparison of the robust stability of the two NDI control laws is attempted by plotting in Fig. 3 the area of the ellipsoids as a function of the amount of parametric uncertainty for each control law. With the PI controller a larger region of attraction is guaranteed for small amounts of uncertainty, suggesting that the presence of the integrator in the outer-loop controller is beneficial.

D. Assessing the Robust Performance of the Proportional NDI Control Law

The methodology used for the robust performance test is the one proposed in Sec. IV, and when it is applied to the quasi-LPV model of Eq. (50) it translates to the following: given the amount of uncertainty in the aerodynamic force and moment ($w_{M_\alpha}=w_{M_\epsilon}=\cdots=w_{Z_\epsilon}=w$), for increasing $\Delta\alpha$ calculate the maximum $\mathcal{L}_2$ norm of the commanded pitch rate q_{com} that is guaranteed to keep the angle of attack in its assumed range and for that class of inputs calculate the $\mathcal{L}_2$-induced gain from q_{com} to q. The attempt here is to evaluate the worst-case degradation in the $\mathcal{L}_2$-induced gain from q_{com} to q from its nominal value (which is one) under the presence of uncertainty and for bounded external inputs.

A solution of the LMI minimization problem of theorem 3.3 gives a guarantee that for all uncertainties satisfying $|\delta_i(t)|\le 1$, and all reference inputs satisfying $\|q_{\text{com}}\|_2^2 < c^2$, the angle of attack will remain in the range $[\alpha_0-\Delta\alpha, \alpha_0+\Delta\alpha]$, assuming that the aircraft was initially flying at its equilibrium state. After the angle-of-attack range is associated with the $\mathcal{L}_2$ norm of the reference input, the LMI problem of theorem 3.4 is solved whose solution implies that $\|q\|_2 < \gamma\|q_{\text{com}}\|_2$ for the considered amount of uncertainty and for all external inputs satisfying $\|q_{\text{com}}\|_2^2 < c^2$.

The NDI control law with a proportional outer-loop controller was tested for five different amounts of uncertainty. The results are

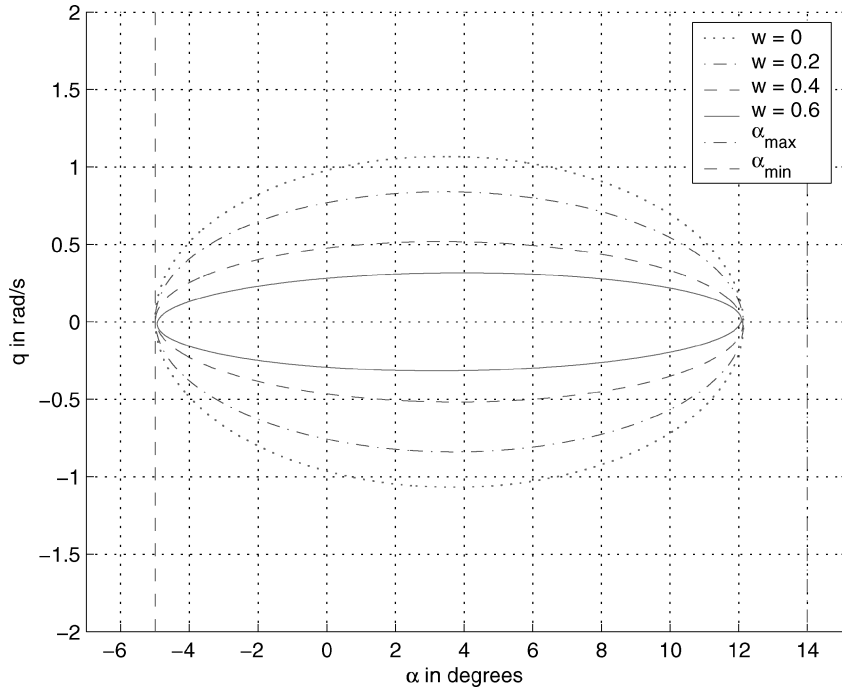

Fig. 2 Comparison of ellipsoids contained in the attraction region for different uncertainty weights with the PI outer-loop controller.

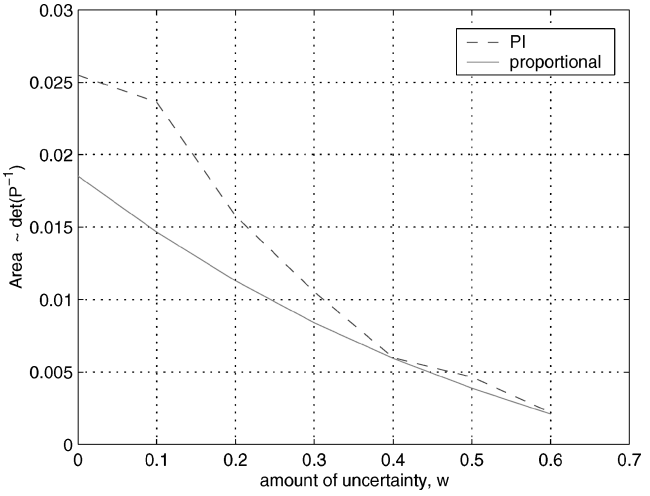

Fig. 3 Comparison of robust stability of PI and proportional NDI control laws with respect to parametric uncertainty.

shown in Fig. 4. Figure 4a shows the guaranteed range of α for external inputs satisfying $\|q_{\text{com}}\|_2 < c$ for various amounts of uncertainty. The dotted line corresponds to the nominal case ($\delta = 0$) and the nominal $\mathcal{L}_2$-induced gain is unity because for perfect inversion the pitch-rate response is $5/(s+5)$. Figure 4b shows the bound on the induced $\mathcal{L}_2$ norm for the specific class of inputs and the specific amount of uncertainty.

In the nominal case the performance of the NDI control law is independent of the scheduling variable because the induced $\mathcal{L}_2$ norm is unity. This is expected because the NDI controller cancels exactly the nonlinearities caused by the angle of attack on the pitch-rate response. In the presence of uncertainty, the performance of the control law degrades both with increasing amounts of uncertainty and with increasing $\mathcal{L}_2$-norm inputs. The following two ways are used to interpret the plots in Fig. 4:

1) Fixed uncertainty: When the $\mathcal{L}_2$ norm of the input is increased, there is an increase in the guaranteed range over which α varies. The upper bound on the $\mathcal{L}_2$-induced gain also increases for larger deviations from the equilibrium α. Hence for a fixed amount of uncertainty the performance is likely to degrade more for larger excursions from the equilibrium flight condition. We can only assess the worst-case degradation of performance. For an example, consider a fixed amount of uncertainty of $w = 0.3$. Looking at the top figure on the line with the square markers, if the $\mathcal{L}_2$ norm of the input is less than 0.1, the angle of attack will deviate by no more than 5 deg from its equilibrium value. Moving vertically downward to the bottom figure, we see that $\|q\|_2 < \gamma \|q_{\text{com}}\|_2 = 1.3 \times 0.1 = 0.13$. If the $\mathcal{L}_2$ norm of the input is doubled to 0.2, the angle of attack will deviate by no more than 10.5 deg, and the $\mathcal{L}_2$ norm of the output will be less than $1.37 \times 0.2 = 0.27$. The degradation in performance with respect to an increase in the $\mathcal{L}_2$ norm of the input is not severe in this example (from 1.3 to 1.37), which suggests that the inversion is working well for uncertainties up to $w = 0.3$. By saying "working well," we mean that similar performance is guaranteed over a large range of the angle of attack, which is the main objective of an NDI control law.

2) Fixed input energy: As the amount of uncertainty increases, there is an increase in the guaranteed region over which α varies. This implies a performance degradation because it is desirable to associate a fixed $\mathcal{L}_2$-norm input with the smallest possible range of α. Furthermore, the bound on the $\mathcal{L}_2$-induced gain also increases with increasing uncertainty.

E. Model Matching Test for Comparing the Performance of NDI Control Laws

The main reason for using NDI in flight control is to achieve a desired, input-output response over the whole of the flight envelope, that is, over large variations in the scheduling variables. It is proposed to examine how the achieved, input-output response deviates from the desired one under the same external excitation and in the presence of uncertainty by using the interconnection in Fig. 5. The energy of the weighted error signal e_w gives an indication of how well the NDI controller can achieve the desired responses for a given energy of the reference signals. The robust performance of the two outer-loop controllers will be compared using the $\mathcal{L}_2$-induced gain from q_{com} to e_w; hence, the robust performance test is applied on a state-space representation of the interconnection in Fig. 5. The test is performed for a fixed amount of uncertainty in the aerodynamic coefficients of $w = 0.3$ for both controllers. The desired pitch-rate response is given by $5/(s+5)$, which is the one achieved under perfect inversion. The error weight is a low-pass filter with cutoff frequency of 7 rad/s, which suggests that we are mainly interested

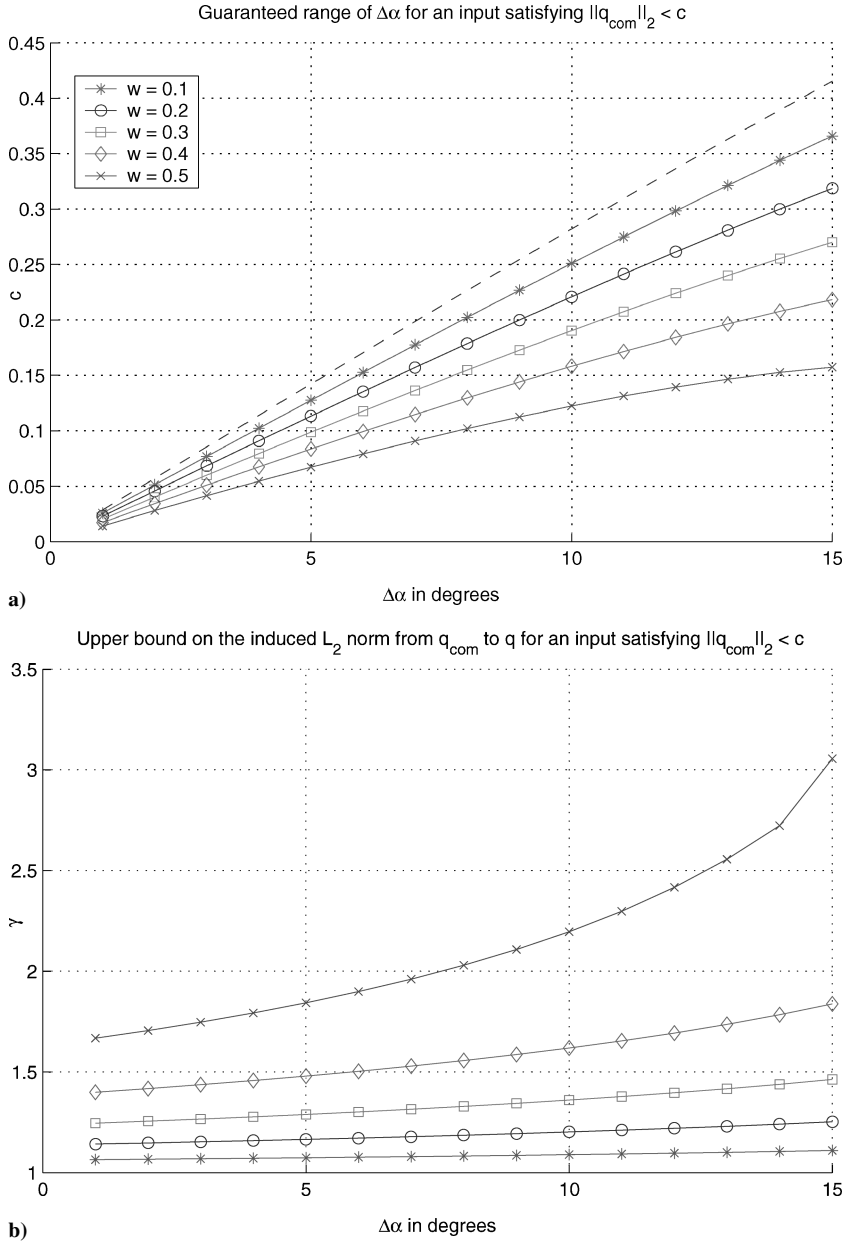

Fig. 4 Results from the performance analysis of the short-period, quasi-LPV model with NDI and a proportional outer-loop controller.

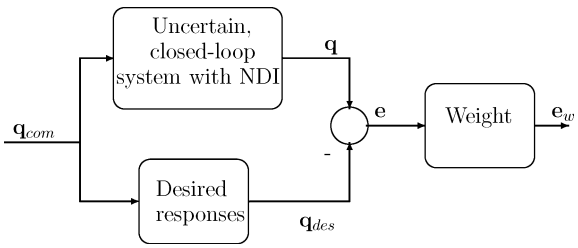

Fig. 5 Interconnection used for comparing the robust performance of NDI control laws.

in the low-frequency error between the two responses. To present the results in a more compact manner, it is proposed to suppress the range of α information and present the plot of the upper bound on the $\mathcal{L}_2$-induced gain directly as a function of the $\mathcal{L}_2$ norm of the reference input as shown in Fig. 6.

The performance of the PI NDI controller is likely to be better (and will not be worse) than that of the proportional NDI controller because the $\mathcal{L}_2$ norm of the weighted error is smaller than that of the

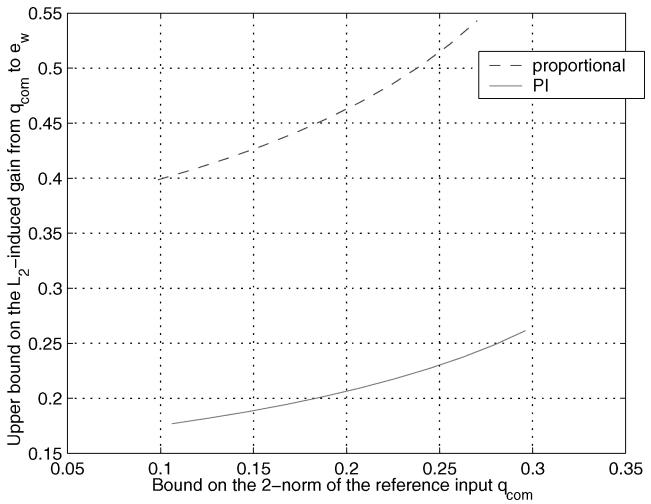

Fig. 6 Comparison of robust performance of two NDI controllers for the same time-varying, parametric uncertainty of $w = 0.3$.

proportional NDI controller over reference inputs of approximately the same $\mathcal{L}_2$ norm.

Furthermore, the variability in performance of the PI controller with respect to the $\mathcal{L}_2$ norm of the reference input is not going to be worse than that of the proportional controller. The presence of the explicit integrator in the PI NDI controller provides better tracking of the pitch-rate references in the presence of parametric uncertainty. The proportional NDI controller cannot cope as well with parametric uncertainty because the mismatch in the inversion destroys the inner-loop integrator response.

VI. Conclusions

Valid and interpretable robust stability and robust performance tests that facilitate the evaluation and comparison of different nonlinear-dynamic-inversion (NDI) control laws without making any simplifications regarding the nonlinear nature of the control laws are derived. The tests provide local stability and performance guarantees because they consider the scheduling variables as part of the state vector of the quasi-linear-parameter-varying model. The robust stability result is interpreted using a subset of the region of attraction of the equilibrium point. The robust performance result is presented using an upper bound on the $\mathcal{L}_2$-induced gain from a reference input of bounded energy to a performance output. The energy of the reference input is related to an ellipsoidal region about the equilibrium point where the scheduling variables are guaranteed to lie. The comparison of two different NDI control laws was performed using the model matching criterion. It was demonstrated that an NDI control law with explicit integral action attains better performance than an NDI control law with simple, proportional action.

Appendix: Proofs of Theorems 3.3 and 3.4

Proof of Theorem 3.3

Proof:

1) The LMI condition (40) implies that

$$A^T(\boldsymbol{x},\boldsymbol{\delta})P + PA(\boldsymbol{x},\boldsymbol{\delta}) < 0, \qquad \forall \boldsymbol{\delta} \in \boldsymbol{\Delta}, \qquad \forall \boldsymbol{x} \in \hat{\boldsymbol{D}} \tag{A1}$$

Because $\boldsymbol{\Delta}$ and $\hat{\boldsymbol{D}}$ are compact sets and A depends continuously on $\boldsymbol{x}$ and $\boldsymbol{\delta}$, it is true that

$$\boldsymbol{x}^T(t)[A^T(\boldsymbol{x}(t),\boldsymbol{\delta}(t))P + PA(\boldsymbol{x}(t),\boldsymbol{\delta}(t))]\boldsymbol{x}(t) < 0 \tag{A2}$$

for any $\boldsymbol{\delta}(t) \in \boldsymbol{F}_\Delta$ and for any trajectory $\boldsymbol{x}(t) \in \hat{\boldsymbol{D}}$ of the autonomous, quasi-LPV model. This implies that $V(\boldsymbol{x}) = \boldsymbol{x}^T P\boldsymbol{x}$ is a valid, quadratic Lyapunov function for the autonomous, quasi-LPV model over the domain $\hat{\boldsymbol{D}}$, and the level surface $\mathcal{E}(P,c)$ is a subset of the region of attraction of the equilibrium point $\boldsymbol{x} = 0$, if it is included in $\hat{\boldsymbol{D}}$. This is satisfied by the condition $\mathcal{E}(P,c) \subset \hat{\boldsymbol{D}}$.

2) The LMI condition (40) implies that

$$\begin{bmatrix}\boldsymbol{x}\\ \boldsymbol{d}\end{bmatrix}^T \begin{bmatrix} A^T(\boldsymbol{x},\boldsymbol{\delta}(t))P + PA(\boldsymbol{x},\boldsymbol{\delta}(t)) & PB(\boldsymbol{x},\boldsymbol{\delta}(t)) \\ B^T(\boldsymbol{x},\boldsymbol{\delta}(t))P & -I \end{bmatrix} \begin{bmatrix}\boldsymbol{x}\\ \boldsymbol{d}\end{bmatrix} < 0 \tag{A3}$$

for any $\boldsymbol{\delta}(t) \in \boldsymbol{F}_\Delta$ and any trajectory $\boldsymbol{x}(t)$ of Eq. (39) that lies in $\hat{\boldsymbol{D}}$. Given that $V(\boldsymbol{x}) = \boldsymbol{x}^T P\boldsymbol{x}$, the preceding is equivalent to

$$\dot{V}(\boldsymbol{x}) < \boldsymbol{d}^T\boldsymbol{d} \tag{A4}$$

for any $\boldsymbol{\delta}(t) \in \boldsymbol{F}_\Delta$ and any trajectory $\boldsymbol{x}(t)$ of Eq. (39) that lies in $\hat{\boldsymbol{D}}$. Integrating from 0 to t $(0 < t \le T)$,

$$\int_0^t \dot{V}(\boldsymbol{x})\,\mathrm{d}t < \int_0^t \boldsymbol{d}^T\boldsymbol{d}\,\mathrm{d}t \Rightarrow V(\boldsymbol{x}(t)) - V(\boldsymbol{x}(0))$$

$$< \int_0^t \boldsymbol{d}^T\boldsymbol{d}\,\mathrm{d}t < \int_0^T \boldsymbol{d}^T\boldsymbol{d}\,\mathrm{d}t < \|\boldsymbol{d}\|_2^2$$

$$\Rightarrow \boldsymbol{x}(t)^T P\boldsymbol{x}(t) < c^2 \qquad \text{for} \qquad 0 < t \le T \tag{A5}$$

given that $\boldsymbol{x}(0) = 0$ and $\|\boldsymbol{d}\|_2^2 < c^2$. This means that up to a time $t = T$ the state lies in the ellipsoid $\boldsymbol{x}^T P\boldsymbol{x} = c^2$ if the assumption $\boldsymbol{x}(t) \in \hat{\boldsymbol{D}}$ is valid. This is indeed the case if the ellipsoid is a subset of $\hat{\boldsymbol{D}}$, which is satisfied by the condition $\mathcal{E}(P,c) \subset \hat{\boldsymbol{D}}$. □

Proof of Theorem 3.4

To prove theorem 3.4, we use a modified version of lemma 2.8 from Ref. 26, which is presented next.

Lemma 4.1 [lemma 2.8 in Ref. 26]: Given that the LPV system in Eq. (21) is quadratically stable, then for $\boldsymbol{d} \in \mathcal{L}_2$, any $\boldsymbol{x}(0) \in \mathbb{R}^n$, and any $\boldsymbol{\rho}(t) \in \boldsymbol{F}_P$,

$$\lim_{t\to\infty} \boldsymbol{x}(t) = 0 \tag{A6}$$

The modification amounts to restricting the applicability of the preceding lemma in a region about the equilibrium point $\boldsymbol{x} = 0$ of the uncertain, quasi-LPV model in Eq. (39), that is, not for inputs of arbitrary energy but for inputs that satisfy $\|\boldsymbol{d}\|_2^2 < c^2$.

Lemma 4.2: Suppose that the uncertain, quasi-LPV model in Eq. (39) is quadratically stable over the ellipsoid $\mathcal{E}(P,c)$. Given that for any $\boldsymbol{\delta}(t) \in \boldsymbol{F}_\Delta$ and for any input such that $\|\boldsymbol{d}\|_2^2 < c^2$, the state trajectory starting from $\boldsymbol{x}(0) = 0$ will remain in the ellipsoid $\mathcal{E}(P,c)$; it is guaranteed that

$$\lim_{t\to\infty} \boldsymbol{x}(t) = 0 \tag{A7}$$

The proof of theorem 3.4 is presented next.

Proof: The LMI condition (41) is equivalent to the existence of a quadratic Lyapunov function $V(\boldsymbol{x}) = \boldsymbol{x}^T P\boldsymbol{x}$ that satisfies

$$\dot{V}(\boldsymbol{x}) + \boldsymbol{e}^T\boldsymbol{e} - \gamma^2\boldsymbol{d}^T\boldsymbol{d} < 0, \qquad \forall \boldsymbol{x}, \boldsymbol{e} \tag{A8}$$

which satisfy the equation of the uncertain, quasi-LPV model with $\boldsymbol{x}(0) = 0$, $\boldsymbol{\delta}(t) \in \boldsymbol{F}_\Delta$, and $\|\boldsymbol{d}\|_2^2 < c^2$. It was proven in theorem 3.3 that under those conditions the trajectory of the system will remain in the ellipsoid $\mathcal{E}(P,c)$ and that the ellipsoid is a subset of the region of attraction of the equilibrium point. Using the result of lemma 4.2, we know that as $t \to \infty$ the state trajectory will tend to zero. Integrating Eq. (58) from $t = 0$ to ∞, we have

$$\int_0^\infty \dot{V}(\boldsymbol{x})\,\mathrm{d}t + \int_0^\infty \boldsymbol{e}^T\boldsymbol{e}\,\mathrm{d}t - \gamma^2\int_0^\infty \boldsymbol{d}^T\boldsymbol{d}\,\mathrm{d}t$$

$$< 0 \Rightarrow \|\boldsymbol{e}\|_2^2 < \gamma^2\|\boldsymbol{d}\|_2^2 \tag{A9}$$

□

Acknowledgments

The work was partially funded by QinetiQ, Ltd., under the MoD Corporate Research Programme "Modelling and Control of Flexible Aircraft," which ended in 2001. Thanks to Yoge Patel and Ian Kaynes from QinetiQ, Ltd., for providing us with the software and technical documentation and for helpful discussions for the nonlinear, aeroservoelastic F/A-18 model.

References

[1]Bugajski, J. D., and Enns, F. D., "Nonlinear Control Law with Application to High Angle of Attack Flight," *Journal of Guidance, Control, and Dynamics*, Vol. 15, No. 3, 1992, pp. 761–767.

[2]Enns, D., Bugajski, D., Hendrick, R., and Stein, G., "Dynamic Inversion: an Evolving Methodology for Flight Control Design," *International Journal of Control*, Vol. 59, No. 1, 1992, pp. 71–91.

[3]Patel, Y., and Smith, P. R., "Translational Motion Control of Vertical Takeoff Aircraft Using Nonlinear Dynamic Inversion," *Journal of Guidance, Control, and Dynamics*, Vol. 21, No. 1, 1998, pp. 179–182.

[4]Smith, P. R., and Berry, A., "Flight Test Experience of a Non-Linear Dynamic Inversion Control Law on the VAAC Harrier," AIAA Paper 2000-3914, Aug. 2000.

[5]Littleboy, D. M., and Smith, P. R., "Using Bifurcation Methods to Aid Nonlinear Dynamic Inversion Control Law Design," *Journal of Guidance, Control, and Dynamics*, Vol. 21, No. 4, 1998, pp. 632–638.

[6]Snell, A., "Decoupling Control with Applications to Flight," *Journal of Guidance, Control, and Dynamics*, Vol. 21, No. 4, 1998, pp. 647–655.

[7]Isidori, A., *Nonlinear Control Systems*, 2nd ed., Springer-Verlag, New York, 1995.

[8]Hauser, J., Sastry, S., and Meyer, G., "Nonlinear Control Design for Slightly Non-Minimum Phase Systems," *Automatica*, Vol. 28, No. 4, 1992, pp. 665-679.

[9]McFarland, B. M., and Hoque, S. M., "Robustness of a Nonlinear Missile Autopilot Designed Using Dynamic Inversion," AIAA Paper 2000-3970, Aug. 2000.

[10]Brinker, J. S., and Wise, K. A., "Stability and Flying Qualities Robustness of a Dynamic Inversion Aircraft Control Law," *Journal of Guidance, Control, and Dynamics*, Vol. 19, No. 6, 1996, pp. 1270–1277.

[11]McFarlane, D., and Glover, K., "A Loop-Shaping Design Procedure Using H_∞ synthesis," *IEEE Transactions on Automatic Control*, Vol. 37, No. 6, 1992, pp. 759–769.

[12]Vinnicombe, G., *Uncertainty and Feedback: H_∞ Loop-Shaping and the ν-Gap Metric*, 1st ed., Imperial College Press, London, 2001.

[13]Papageorgiou, G., and Hyde, R. A., "Analysing the Stability of NDI-Based Flight Controllers with LPV Methods," AIAA Paper 2001-4039, Aug. 2001.

[14]Glover, K., Vinnicombe, G., and Papageorgiou, G., "Guaranteed Multi-Loop Stability Margins and the Gap Metric," *Proceedings of the 2000 IEEE Conference on Decision and Control*, Sydney, Australia, 2000, pp. 4084, 4085.

[15]Schumacher, C. J., and Khargonekar, P. P., "Stability Analysis of a Missile Control System with a Dynamic Inversion Controller," *Journal of Guidance, Control, and Dynamics*, Vol. 21, No. 3, 1998, pp. 508–515.

[16]Morton, B., Enns, D., and Zhang, B., "Stability of Dynamic Inversion Control Laws Applied to Nonlinear Aircraft Pitch-Axis Models," *International Journal of Control*, Vol. 63, No. 1, 1996, pp. 1–25.

[17]Shamma, J. S., and Athans, M., "Analysis of Gain Scheduled Control for Nonlinear Plants," *IEEE Transactions on Automatic Control*, Vol. 35, No. 8, 1990, pp. 898–907.

[18]Tsourdos, A., Leith, D. J., Leithead, W. E., and White, B. A., "A Velocity-Based Framework for the Robust Stability Analysis of Dynamic Inversion Flight Controllers," *Proceedings of the American Control Conference*, Vol. 5, 2001, pp. 3341–3345.

[19]Shamma, J. S., and Cloutier, R. J., "Gain-Scheduled Missile Autopilot Design Using Linear Parameter Varying Transformations," *Journal of Guidance, Control, and Dynamics*, Vol. 16, No. 2, 1993, pp. 256–263.

[20]Huang, Y., and Jadbabaie, A., "Nonlinear H_∞ Control: An Enhanced Quasi-LPV Approach," *Proceedings of the 14th IFAC World Congress*, Beijing, 1999, pp. 85–90.

[21]Papageorgiou, C., "Robustness Analysis of Nonlinear Dynamic Inversion Control Laws for Flight Control Applications," Ph.D. Dissertation, Engineering Dept., Cambridge Univ., 2003.

[22]Tan, W., "Applications of Linear Parameter-Varying Control Theory," M.S. Thesis, Dept. of Mechanical Engineering, Univ. of California, Berkeley, CA, May 1997.

[23]Marcos, A., and Balas, G. J., "Development of Linear Parameter-Varying Models for Aircraft," *Journal of Guidance, Control, and Dynamics*, Vol. 27, No. 2, 2004, pp. 218–228.

[24]Khalil, H. K., *Nonlinear Systems*, Prentice–Hall, Upper Saddle River, NJ, 1996.

[25]Boyd, S., El Ghaoui, L., Feron, E., and Balakrishnan, B., *Linear Matrix Inequalities in System and Control Theory*, Society of Industrial and Applied Mathematics, 1994.

[26]Becker, G., and Packard, A., "Robust Performance of Linear Parametrically Varying Systems Using Parametrically-Dependent Linear Feedback," *Systems and Control Letters*, Vol. 23, No. 3, 1994, pp. 205–215.

[27]Scherer, C., and Weiland, S., "Lecture Notes on Linear Matrix Inequalities in Control," Dutch Inst. of Systems and Control, 2000.

[28]Gahinet, P., Nemirovski, A., Laub, A. J., and Chilali, M., *LMI Control Toolbox*, May 1995.

[29]Etkin, B., and Reid, L. D., *Dynamics of Flight, Stability and Control*, Wiley, New York, 1995.

[30]Standen, P., "Consistent Nonlinear F-18 Aeroservoelastic Model," Stirling Dynamics, Ltd., Tech. Rept. SDL-649-TR-1, Aug. 2000.